

Proceeding Paper

A Novel Synthetic Approach of Functionalised GO and CNT to Nanocomposite Containing Active Nanostructured Fillers for Classical Isocyanate Curing [†]

Lina Jadhav ¹, Rahul Patil ¹, Nikhil Borane ¹, Satyendra Mishra ¹, Ganapati D. Yadav ², Dipak B. Patil ³ and Vikas Patil ^{1,2,*} 

¹ University Institute of Chemical Technology, Kavayitri Bahinabai Chaudhari North Maharashtra University, Jalgaon 425001, India; lina.jadhav345@gmail.com (L.J.); rahul92ppatil@gmail.com (R.P.); nikhilborane1990@gmail.com (N.B.); profsm@rediffmail.com (S.M.)

² Institute of Chemical Technology, Mumbai 400019, India; gdyadav@yahoo.com

³ Departamento de Química, División de Ciencias Naturales y Exactas, Campus Guanajuato, Universidad de Guanajuato, Noria Alta S/N, Guanajuato 36050, Mexico; patildip98@gmail.com

* Correspondence: vikasudct@gmail.com

[†] Presented at the 25th International Electronic Conference on Synthetic Organic Chemistry, 15–30 November 2021; Available online: <https://ecsoc-25.sciforum.net/>.

Abstract: A novel synthetic method has been developed by utilizing the chemical reactivity of functionalized graphene and CNT with a covalent combination of chemically diverse GO/FCNT and toluene diisocyanate, thereby yielding a synergistic polymer nanocomposite. Comprehensive composite material has simultaneous covalent, as well as π - π , interactions confirming sp²-hybridized frameworks of graphene oxide and MWCNTs by Raman absorption spectra at 1345 and 1590 cm⁻¹ of D and G bands, respectively. Toluene diisocyanate and GO/FCNT inspired polymeric formulation was obtained by the classical curing reaction initiated by ultrasound sonication. This method allowed 50 wt.% doping of GO/FCNT without segregation and ensured good adhesion to the low steel surface. The large surface area and morphological character of GO and FCNT by SEM and TEM ensure stable and dispersed integrated molecules. This has advantages over high-temperature and hazardous curing reaction, and overcomes the problem of graphene exfoliation. It also does not allow CNT slipping within the bundle, which can cause falling apart at higher concentration.

Keywords: graphene; CNT; isocyanate; curing; filler; nanostructured



Citation: Jadhav, L.; Patil, R.; Borane, N.; Mishra, S.; Yadav, G.D.; Patil, D.B.; Patil, V. A Novel Synthetic Approach of Functionalised GO and CNT to Nanocomposite Containing Active Nanostructured Fillers for Classical Isocyanate Curing. *Chem. Proc.* **2022**, *8*, 33. <https://doi.org/10.3390/ecsoc-25-11679>

Academic Editor: Julio A. Seijas

Published: 13 November 2021

Publisher's Note: MDPI stays neutral with regard to jurisdictional claims in published maps and institutional affiliations.



Copyright: © 2021 by the authors. Licensee MDPI, Basel, Switzerland. This article is an open access article distributed under the terms and conditions of the Creative Commons Attribution (CC BY) license (<https://creativecommons.org/licenses/by/4.0/>).

1. Introduction

Complimentary properties of organic and inorganic materials are combined to generate a new composite material, generating new hybrid composite materials. The new hybrid composite material has combined properties of both organic and inorganic compounds [1]. Before compositing two chemically distinct species, synergy was installed by functionalisation of an essential component [2]. Functionalisation permits chemical response, which improves mechanical, thermal, electrical, UV resistance, and abrasion properties in hybrid organic-inorganic materials [3,4]. In polymer nano-composite, lack of covalent interactions allows exfoliation of filler material into the complex matrix. This problem is further overcome by chemical functionalisation and the subsequent covalent combination of nanostructure filler into the polymeric matrix [5]. The isocyanate is a functional species ready to be combined with chemically modified filler material, thereby enhancing the intrinsic properties of the final composite material for application. Consequently, the final composite material has reduced hydrophilic properties, due to the utilization of hydroxyl and acid functionality of the filler, and forms new hydrophobic amide and carbamate ester linkages. As a result of this, it is no longer exfoliated into the solvent, helping in the stably dispersed

constructive formulation. Segregation has been observed at very low concentration of 0.1 vol% of graphene as filler in polystyrene. It was evidenced that there is no constructive attraction between filler and polymer. Physical laying of filler into the polymer matrix immediately segregates at high concentration [6,7].

Owing to the strong and inbuilt sustainable properties of CNT it is able to retain five to ten times more load than steel. Compared to steel, CNT inclusion creates magical properties due to the active large surface, 1/6 weight, 50–100 G Pa tensile strength and 1–2 T Pa modulus [8–11]. Next generation performing materials have multifunctionality due to CNT and graphene, with unique mechanical, thermal, and surface properties. CNT and graphene polymer nanocomposite coating binds synergy of film thickness, interparticle spacing of the filler and thermomechanical properties [12]. Further 2 wt.% SWNTs added to the coating results in 125% thermal conductivity and 3.5-factor increase in Vickers hardness. To date, the use of CNTs and graphene nanocomposites has been limited by challenges in processing, dispersion, and their prohibitively high cost. Ajayan et al. demonstrated the preparation of epoxy composite by dispersing multiwall nanotubes in the epoxy under ultrasonic force [13]. Higher concentrations of more than 5% nanotubes in composite slip within the bundle and fall apart, which is responsible for poor load transfer within the cured composite. This was supported by Raman spectra, tension and compression analysis [14]. Sandler et al. tried to improve dispersion of SWNTs by ultrasonic application and intense stirring. A slight improvement was observed in the configuration of nanotubes but it still failed on the millimeter scale [15]. Irrespective of the sliding of the SWNTs, into the ropes, continuous increase in Young's modulus was observed with respect to increasing concentration. Improper configuration slides SWNTs into the rope, and bending of the rope decreases mechanical strength [16]. Furthermore, surfactants were also used to improve the dispersion of nanotubes in epoxy. This retained the mechanical strength of the composition [17]. Surfactant and ultrasonically dispersed epoxy-nanotube composition appear to be finely dispersed, but microscopic. Analysis found there to be inhomogeneous dispersion in the composition [18]. To overcome this, an integrated system was developed upon functionalization of GO/FCNT, and exploited to induce curing of diisocyanate. The composite was used as a corrosion resistive coating on low alloy steel [19,20]. Loading of 50 wt.% filler achieved stable, mechanically strong and highly dispersed FCNT/GO isocyanate composite for surface coating [21,22].

2. Experimental

2.1. Materials and Methods

Single-walled carbon nano tubes were purchased from Alfa Aesar. Graphene and toluene diisocyanate precursor were purchased from Sigma Aldrich. Anhydrous THF was used as a solvent in this process and functionalization was done by using NaNO_3 , KMnO_4 , and H_2SO_4 in deionized water. Low alloy steel for coating was used from a local supplier in Mumbai, India. Functionalization of CNT and Graphene was performed by the Hummer's method [23]. Further composites were prepared and obtained fine dispersion. Surface coating of nano-composite on low-alloy steel was performed by a simple bar coating method. Formulations containing 50, 25, 10, 5 wt.% of filler content of average precision film thickness were obtained.

2.2. Characterization of Structure and Surface Morphology

IRRA (infrared reflection absorption) spectra were utilized for the characterisation of functional modification in CNT and graphene. IRRA was carried out by a Perkin Elmer 100 FT-IR spectrophotometer with Olympus BX51 microscope attachment. Raman spectroscopy was performed by Horiba Jobin Yvon Labram HR system with 514.5 nm laser excitation. The surface morphology of composites was investigated by scanning electron microscopy (SEM) on a Hitachi SU-70 instruments, operated at accelerating voltage of 20 kV. Transmission electron microscopy (TEM) was used for dispersion study of the composite by a JEOL-2010 instrument operated at 200 kV and 100 mA equipment. Film thickness was

measured by shin equipment, Mumbai. The rate of corrosion was detected by deep method in 3.5% NaCl solution for 2160 h.

3. Results and Discussion

3.1. Functionalisation, Dispersion of FCNT/GO and Curing of Isocyanate

The overall strategy shown in Figure 1 depicts dispersion of active carbon material in isocyanate. The accessible functional groups on the surface of carbon material induce cross-linking to di-isocyanate. Initial reports on a high degree of functionalisation, followed by fluorination, were employed to obtain large dispersion and mechanical strength in epoxy nanocomposite [24]. Thereby acid and fluorine covalently bind with active epoxy. An acid functional group readily forms ester while diamine becomes an active spacer and readily replaces side wall fluorine [24,25]. Here toluene di-isocyanate was employed as an active crosslinking bifunctional spacer between two nano-materials. The induced cross-linking was materialised by excessive probe sonication. The overall challenge of nano particle segregation and constant dispersion in a solvent was overcome by reactive sites, both on the nanomaterial and the diisocyanate precursor.

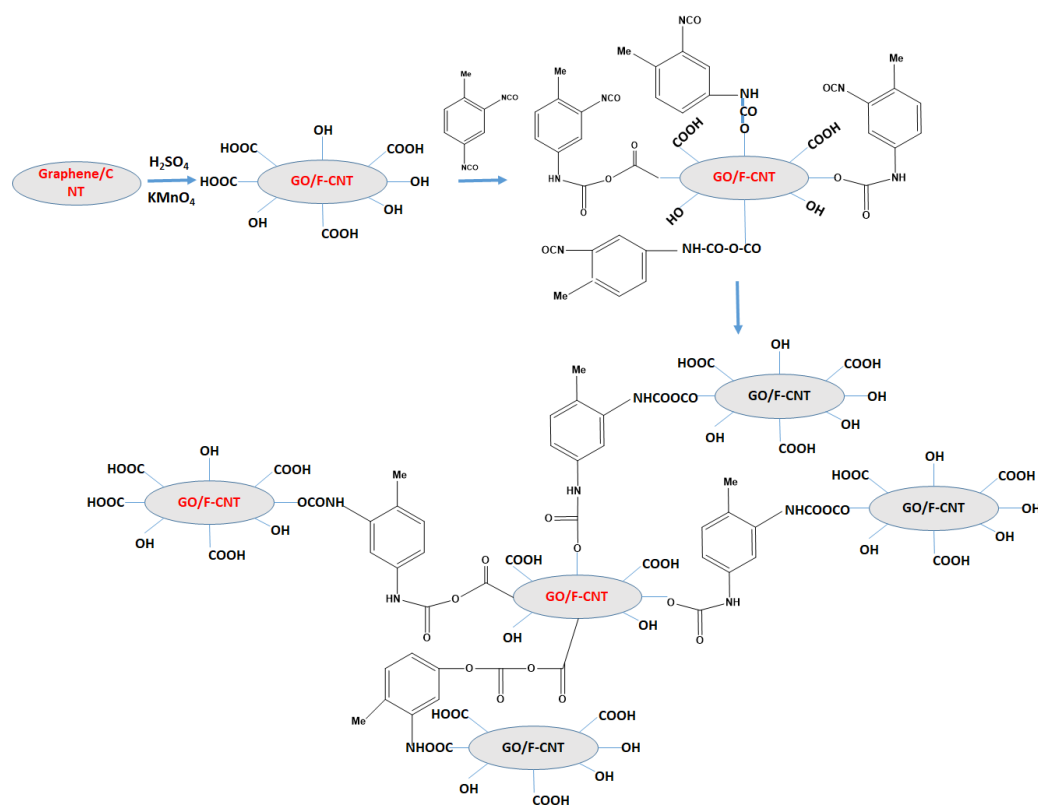


Figure 1. Schematic of graphene CNT functionalization, composite formation with toluene diisocyanate.

Structural changes in the composite were noted and analyzed by characteristic IRRA peaks. GO@isocyanate showed a specific broad absorption peak at 3407 cm^{-1} (Figure 2b). While CNT@isocyanate showed relatively small absorbance in the same region (Figure 2a). Separate peaks at 3298 cm^{-1} and 3528 cm^{-1} arose in toluene diisocyanate and confirmed a urethane link $\text{N}=\text{C}$ (Figure 2a). Broad absorbance at 3400 cm^{-1} was absent completely in the pure toluene di-isocyanate. In pure toluene di-isocyanate, C-H stretching absorption spectra were observed at 2987 cm^{-1} and further strongly recognised in both composites of GO/FCNT@isocyanate, due to the influence of non-stacking with the surface, and non-hydrogen bonding. Sharp absorption bands were observed in the fingerprint region, whereas, for pure toluene di-isocyanate, a bundle of peaks was observed in this region. Peaks were commonly observed at close to 1377 cm^{-1} in all spectra, explaining

the $-\text{CH}_3$ group of toluene diisocyanate carried forward in composite formation. The aromatic nature of toluene diisocyanate compound was confirmed by absorption peaks at 1170 cm^{-1} and 1534 cm^{-1} . The IR absorption spectra at 1130 cm^{-1} for GO@isocyanate, and 1164 cm^{-1} for FCNT@isocyanate, corresponded to the C-C-O ether linkage. Absorption at 934 cm^{-1} for the GO@isocyanate and 927 cm^{-1} for FCNT@isocyanate is C-H stretch vibrations of methylene were attributed to at least one aliphatic fragment or center. The broad peak at 2291 cm^{-1} was observed for the toluene diisocyanate, which is a specific isocyanate bond confirmation further, which completely vanished in both GO@isocyanate and FCNT@isocyanate composites. It confirmed that the purpose of curing the isocyanate by nano-imbedded particles, like FCNT and GO, was successfully achieved. Significant change was observed in the IRRA absorption spectra of the surface, incorporated with active functional nanoparticles and only isocyanate as such.

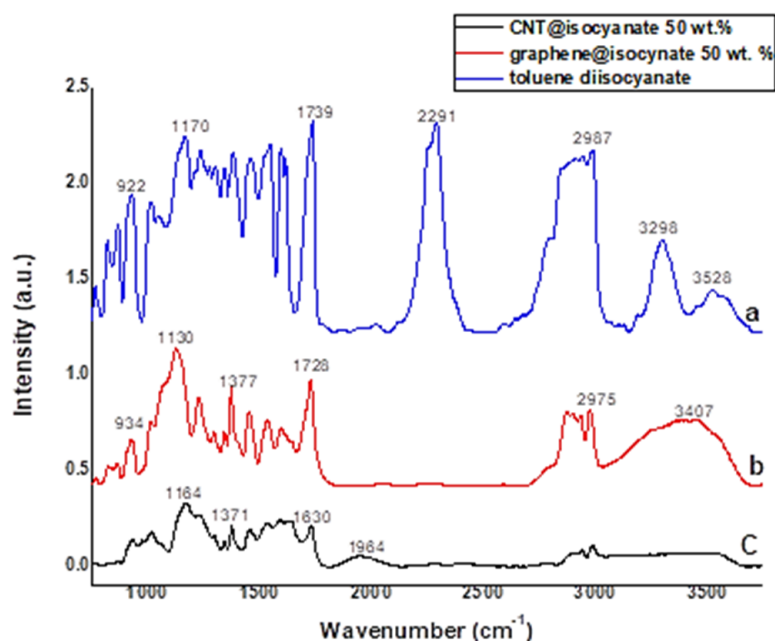


Figure 2. IRRA spectra (a) toluene di-isocyanate without doping on steel surface (b) GO@isocyanate 50 wt.% (c) FCNT@isocyanate 50 wt.%.

3.2. Interface Chemistry between GO/FCNT@isocyanatematrix

Kozłowski and Jones et al. suggested synergy in a two phasic system was due to interfacial physical π - π and covalent chemical compatibility [26,27]. The interfaces of GO/FCNT become more compatible by simultaneously strong covalent and π - π interaction with the diisocyanate host. Few covalently unbounded GO/FCNT interfaces have strong π - π interaction and remain dispersed without agglomeration (Figure 1). In situ reaction helps in non-agglomeration and phase separation of the polymer and GO/FCNT. Hydroxyl and carboxylic acid functional groups grafted onto the GO/FCNT provide a way for in situ chemical integration of the GO/FCNT into the isocyanate system.

As mentioned previously, simultaneously strong covalent and π - π interactions are involved in facilitating the interfaces between the nanostructured filler and isocyanate matrix. Electron microscopy further corroborated fine dispersion of the nanostructure carbonaceous material in the isocyanate. The properly dispersed GO and MWCNTs over isocyanate in the coating is shown by SEM images in Figure 3 on low-alloy steel. The sample was cryo-fractured in liquid nitrogen and a cross section SEM image was captured, which indicates well dispersed oxidised MWCNTs and GO. There was no clue for the segregation of MWCNTs and GO in SEM. Hemispherical caps of the MWCNTs were observed. The evidence of covering of the polymeric matrix to nanomaterial was also observed in SEM. Figure 3a depicts MWCNT@isocyanate, while GO@Isocyanate is shown in Figure 3a. The

swelling of the polymeric matrix observed with nanomaterials and a rough surface were observed in the coating. Similarly, Figure 3d shows graphene oxide sheets embedded within the isocyanate matrix. The carbon nanomaterial on isocyanate was evaluated with TEM images. Figure 4a,b show complete dispersion of the separated GO sheet and oxidised nanotubes in isocyanate. In Figure 4b's TEM of high resolution, complete covering was observed i.e., wrapping of the polymeric matrix to the MWCNTs, indicating similar observation of graphene oxide wrapping in isocyanate matrix (Figure 4c). Despite extensive functionalisation, the crystalline order of some graphene oxide was preserved, shown in Figure 4d in selected area electron diffraction pattern. The sp²-hybridized frameworks of graphene oxide and MWCNTs were confirmed by absorption in Raman spectra at 1345 and 1590 cm⁻¹ of D and G bands, respectively (Figure 5). It was noted that the positions of the D and G bands are finely disturbed while compositing with the isocyanate matrix. The intensity of the D and G bands are much more affected before and after compositing. In the isocyanate matrix, the intensity of the G band was slightly declined rather than in MWNTs alone. Further the D band becomes comparably intensive with the G band for graphene oxide in isocyanate, and comparable increase in intensity of the G band for MWCNTs was observed. As expected, after functionalisation, intensity of the 2D band no significant change in the MWCNTs was observed, due to the disruption of p-conjugation arising from the double bond resonance process, which was no more promising for graphene oxide. The compatibility of nanostructure filler and host matrix was due to the dual modality of the covalent bond and π - π interactions, illustrated in Figures 1, 3 and 5. There are other ways to have compatibility in nanostructure filler and a polymeric matrix. To the best of our knowledge, and with reference to literature, this is the sole example for coating application using graphene oxide and oxidised MWCNTs as curing agents.

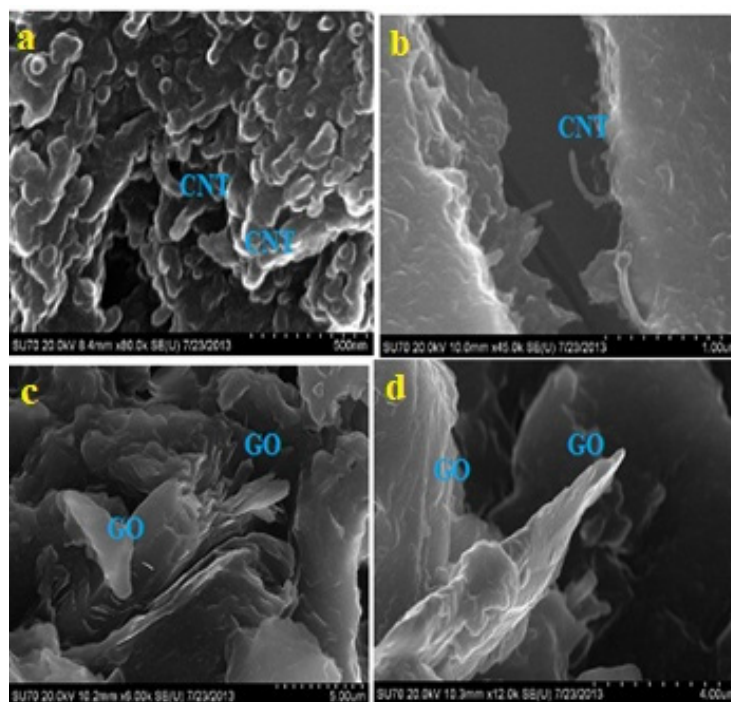


Figure 3. Cross section SEM images of (a,b) for GO@isocyanate 50 wt.% (c,d) for FCNT@isocyanate 50 wt.%.

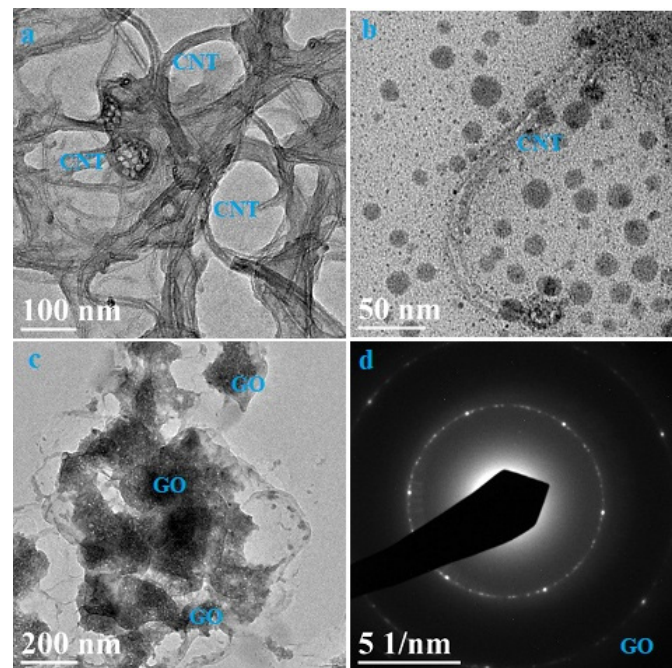


Figure 4. TEM (a,b) for FCNT@isocyanate 50 wt.% (c) for GO@isocyanate 50 wt.% and (d) image is selected area electron diffraction (SAED) pattern acquired for the 50 wt.% graphene-oxide@isocyanate composite.

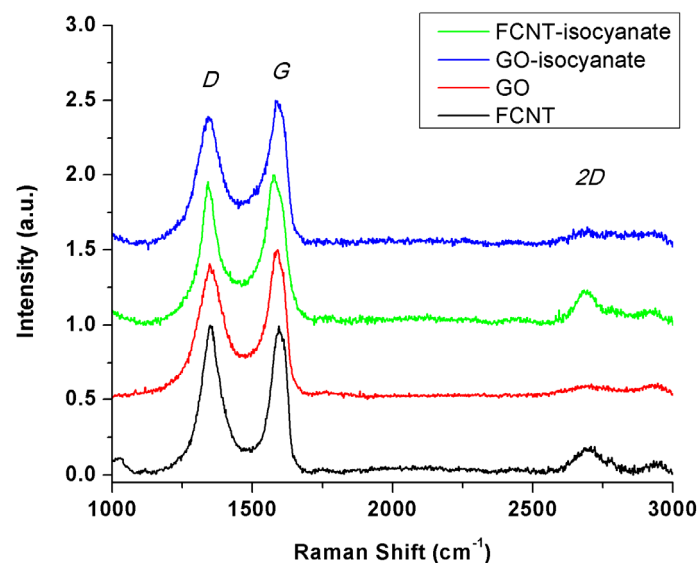


Figure 5. Raman spectra of pure GO and FCNT and isocyanate composite with GO and FCNT.

3.3. Corrosion Inhibition Endowed by Nanocomposite Coatings

The digital photograph in Figure 6 depicts exposer of 50, 25, 10, and 5 wt.% GO/FCNT@isocyanate in 3.5% NaCl solution for 2160 h. Strong resistance to corrosion was observed at higher loading, i.e., 25 and 50 wt.%, while at 5 and 10 wt.% significant corrosion was observed after long exposer to salt solution.

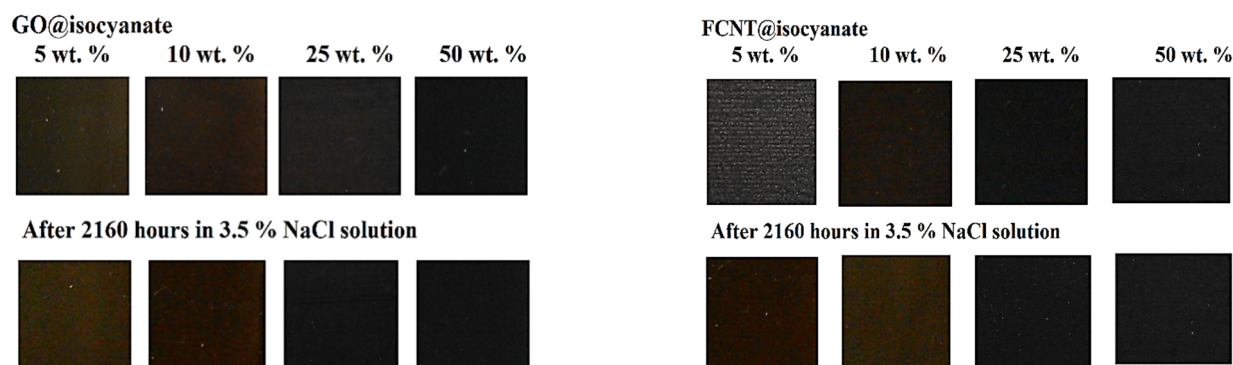


Figure 6. Corrosion measurement in salt water (NaCl 3.5%) of GO@isocyanate and FCNT@isocyanate.

3.4. Mechanical Properties

Mechanical properties of isocyanate composites have been tested for impact resistance, pencil hardness, scratch hardness, adhesion, cracking resistance and flexibility. The results are summarized in Table 1. It shows good resistance to cracking (flexibility). The pencil hardness is 5H for all the coating, except 5 wt.% GO/FCNT@isocyanate. Similarly, adhesion of coating was fairly good at meeting the standards. Adhesion of 5 wt.% GO/FCNT@isocyanate was 4B, while the rest of the coating samples had 5B. Further, all the samples were found to have good resistance over scratch hardness. The average scratch hardness was 2.9 Kg.

Table 1. Mechanical properties of polymer films with various %wt of GO/FCNT@isocyanate.

| | %Weight of GO/FCNT@isocyanate | | | | | | | |
|-----------------------|-------------------------------|------|------|------|-----------------|------|------|------|
| | GO@isocyanate | | | | FCNT@isocyanate | | | |
| | 5 | 10 | 25 | 50 | 5 | 10 | 25 | 50 |
| Impact Resistance | Pass | Pass | Pass | Pass | Pass | Pass | Pass | Pass |
| Pencil hardness | 4H | 5H | 5H | 5H | 5H | 5H | 5H | 5H |
| Flexibility | Pass | Pass | Pass | Pass | Pass | Pass | Pass | Pass |
| Adhesion | 3B | 5B | 5B | 5B | 5B | 5B | 5B | 5B |
| Scratch Hardness (Kg) | 2.8 | 2.9 | 3.0 | 3.0 | 2.8 | 2.9 | 2.9 | 3.0 |

4. Conclusions

The concept of a chemical reaction between two phase materials GO/FCNT with isocyanate was executed and utilized as a corrosion resistive coating material. Chemically activated carbonaceous nanomaterial was integrated into the core structure of the polymer matrix, united by covalent, as well as π - π , chemical combination. It allows loading about 50 wt.% of nanofiller into polymer matrix to deliver better surface and mechanical properties. The general problem at high loading of graphene exfoliation and sleeping of nanotubes was overcome by the covalent bonding approach and formed a stable dispersion.

Author Contributions: V.P. is contributed for conceptualization, L.J. for experimental part, R.P. and N.B. for methodology, G.D.Y. and S.M. for supervision and D.B.P. for original draft preparation. All authors have read and agreed to the published version of the manuscript.

Funding: This research received no external funding.

Institutional Review Board Statement: Experimental part does not involve human or animal study.

Informed Consent Statement: Not Applicable.

Data Availability Statement: Not applicable.

Acknowledgments: Vikas Patil is thankful to UGC for Faculty Recharge Program and Start Up grant and INDO-US Science and Technology Forum for Post-Doctoral Visiting Fellowship. We thank group of Sarabjit Banerjee and Robert Dennis for analytical support at University at Buffalo. Vikas Patil is thankful to DST India for Waste Management Technology (WMT) project of Technology Transfer Division (TTD) (DST/TDT/WMT/Agwaste/2021/09(G) & (C). Lina Jadhav is thankful to MHRD TEQIP-III for financial support.

Conflicts of Interest: We confirm that there are no conflict of interest associated with this publication and there has been no significant financial support for this work that could have influenced its outcome.

References

1. Shankar, A.R.; Kuma, S.; Piana, F.; Mičušík, M.; Pionteck, J.; Banerjee, S.; Voit, B. Preparation of graphite derivatives by selective reduction of graphite oxide and isocyanate functionalization. *Mater. Chem. Phys.* **2016**, *182*, 237–245.
2. Haghdadeh, P.; Ghaffari, M.; Ramezanzadeh, B.; Bahlakeh, G.; Saeb, M.R. Polyurethane coatings reinforced with 3-(triethoxysilyl)propyl isocyanate functionalized graphene oxide nanosheets: Mechanical and anti-corrosion properties. *Prog. Org. Coat.* **2019**, *136*, 105243. [[CrossRef](#)]
3. Maher, M.; Alrashed Mark, D.; Soucek Sadhan, C. Jana Role of graphene oxide and functionalized graphene oxide in protective hybrid coatings. *Prog. Org. Coat.* **2019**, *134*, 197–208.
4. Adak, B.; Joshi, M.; Butola, B.S. Polyurethane/functionalized-graphene nanocomposite films with enhanced weather resistance and gas barrier properties. *Compos. Part B Eng.* **2019**, *176*, 107303. [[CrossRef](#)]
5. Stankovich, S.; Piner, R.D.; Nguyen, S.T.; Ruoff, R.S. Synthesis and exfoliation of isocyanate-treated graphene oxide nanoplatelets. *Carbon* **2006**, *44*, 3342–3347. [[CrossRef](#)]
6. Chen, G.; Weng, W.; Wu, D.; Wu, C. PMMA/graphite nanosheets composite and its conducting properties. *Eur. Polym. J.* **2003**, *39*, 2329–2335. [[CrossRef](#)]
7. McLachlan, D.S.; Chiteme, C.; Park, C.; Wise, K.E.; Lowther, S.E.; Lillehei, P.T.; Siochi, E.J.; Harrison, J.S. B AC and DC percolative conductivity of single wall carbon nanotube polymer composites. *J. Polym. Sci.* **2005**, *43*, 3273. [[CrossRef](#)]
8. Berber, S.; Kwon, Y.K.; Tomanek, D. Unusually High Thermal Conductivity of Carbon Nanotubes. *Phys. Rev. Lett.* **2000**, *84*, 4613. [[CrossRef](#)]
9. Lourie, O.; Wagner, H.D. Evaluation of Young's modulus of carbon nanotubes by micro-Raman spectroscopy. *J. Mater. Res.* **1998**, *13*, 2418–2422. [[CrossRef](#)]
10. Walters, D.A.; Ericson, L.M.; Casavant, M.J.; Liu, J.; Colbert, D.T.; Smith, K.A.; Smalley, R.E. Elastic strain of freely suspended single-wall carbon nanotube ropes. *Appl. Phys. Lett.* **1999**, *74*, 3803. [[CrossRef](#)]
11. Andrews, R.; Jacques, D.; Rao, A.M.; Rantell, T.; Derbyshire, F.; Chen, Y.; Chen, J.; Haddon, R.C. Nanotube composite carbon fibers. *Appl. Phys. Lett.* **1999**, *75*, 1329. [[CrossRef](#)]
12. Bansal, A.; Yang, H.; Li, C.; Cho, K.; Benicewicz, B.C.; Kumar, S.K.; Schadler, L.S. Quantitative equivalence between polymer nanocomposites and thin polymer films. *Nat. Mater.* **2005**, *4*, 693–698. [[CrossRef](#)] [[PubMed](#)]
13. Schadler, L.S.; Giannaris, S.C.; Ajayan, P.M. Load transfer in carbon nanotube epoxy composites. *Appl. Phys. Lett.* **1998**, *73*, 3842. [[CrossRef](#)]
14. Ajayan, P.; Schadler, L.; Giannaris, C.; Rubio, A. Single-walled carbon nanotube–polymer composites: Strength and weakness. *Adv. Mater.* **2000**, *12*, 750. [[CrossRef](#)]
15. Sandler, J.; Shaffer, M.S.P.; Prasse, T.; Bauhofer, W.; Schulte, K.; Windle, A.H. Development of a dispersion process for carbon nanotubes in an epoxy matrix and the resulting electrical properties. *Polymer* **1999**, *40*, 5967. [[CrossRef](#)]
16. Vaccarini, L.; Desarmot, G.; Almairac, R.; Tahir, S.; Goze, C.; Bernier, P. Reinforcement of an epoxy resin by single walled nanotubes. *AIP Conf. Proc.* **2000**, *544*, 521.
17. Gong, X.; Liu, J.; Baskaran, S.; Voise, R.D.; Young, J.S. Surfactant-assisted processing of carbon nanotube/polymer composites. *Chem. Mater.* **2000**, *12*, 1049. [[CrossRef](#)]
18. Kamae, T.; Drzal, L.T. Carbon fiber/epoxy composite property enhancement through incorporation of carbon nanotubes at the fiber–matrix interphase—Part I: The development of carbon nanotube coated carbon fibers and the evaluation of their adhesion. *Compos. Part A Appl. Sci. Manuf.* **2012**, *43*, 1569–1577. [[CrossRef](#)]
19. Cui, G.; Bi, Z.; Zhang, R.; Liu, J.; Yu, X.; Li, Z. A comprehensive review on graphene-based anti-corrosive coatings. *Chem. Eng. J.* **2019**, *373*, 104–121. [[CrossRef](#)]
20. Ding, R.; Chen, S.; Lv, J.; Zhang, W.; Zhao, X.; Liu, J.; Wang, X.; Gui, T.; Li, B.; Tang, Y.; et al. Study on graphene modified organic anti-corrosion coatings: A comprehensive review. *J. Alloy. Compd.* **2019**, *806*, 611–635. [[CrossRef](#)]
21. Parhizkar, N.; Shahrabi, T.; Ramezanzadeh, B. Journal of the Synthesis and characterization of a unique isocyanate silane reduced graphene oxide nanosheets; Screening the role of multifunctional nanosheets on the adhesion and corrosion protection performance of an amido-amine cured epoxy composite. *Taiwan Inst. Chem. Eng.* **2018**, *82*, 281–299. [[CrossRef](#)]

22. Parhizkar, N.; Ramezanzadeh, B.; Shahrabi, T. Corrosion protection and adhesion properties of the epoxy coating applied on the steel substrate pre-treated by a sol-gel based silane coating filled with amino and isocyanate silane functionalized graphene oxide nanosheets. *Appl. Surf. Sci.* **2018**, *439*, 45–59. [[CrossRef](#)]
23. Patil, V.; Dennis, R.V.; Rout, T.K.; Banerjee, S.; Yadav, G.D. Graphene oxide and functionalized multi walled carbon nanotubes as epoxy curing agents: A novel synthetic approach to nanocomposites containing active nanostructured fillers. *RSC Adv.* **2014**, *4*, 49264–49272. [[CrossRef](#)]
24. Stevens, J.L.; Huang, A.Y.; Peng, H.; Chiang, I.W.; Khabashesku, V.N.; Margrave, J.L. Sidewall Amino-Functionalization of Single-Walled Carbon Nanotubes through Fluorination and Subsequent Reactions with Terminal Diamines. *Nano Lett.* **2003**, *3*, 331–336. [[CrossRef](#)]
25. Voevodin, N.N.; Balbyshev, V.N.; Khobaib, M.; Donley, M.S. Nanostructured sol-gel derived conversion coatings based on epoxy-and amino-silanes. *Prog. Org. Coat.* **2003**, *47*, 207–213.
26. Kozlowski, C.; Sherwood, P.M.A. X-ray photoelectron spectroscopic studies of carbon fiber surfaces VIII—A comparison of type I and type II fibers and their interaction with thin resin films. *Carbon* **1987**, *25*, 751–760. [[CrossRef](#)]
27. Jones, C. The chemistry of carbon fibre surfaces and its effect on interfacial phenomena in fibre/epoxy composites. *Compos. Sci. Technol.* **1991**, *42*, 275–298. [[CrossRef](#)]